

RESEARCH PAPER

## ZnO nanofluids for the improved cytotoxicity and cellular uptake of doxorubicin

Safoura Soleymani<sup>1</sup>, Raziieh Jalal<sup>1,2\*</sup>

<sup>1</sup>Department of Chemistry, Faculty of Science, Ferdowsi University of Mashhad, Mashhad, Iran

<sup>2</sup>Cell and Molecular Biotechnology Research Group, Institute of Biotechnology, Ferdowsi University of Mashhad, Mashhad, Iran

### ABSTRACT

**Objective(s):** Combination anticancer therapy holds promise for improving the therapeutic efficacy of chemotherapy drugs such as doxorubicin (DOX) as well as decreasing their dose-limiting side effects. Overcoming the side effects of doxorubicin (DOX) is a major challenge to the effective treatment of cancer. Zinc oxide nanoparticles (ZnO NPs) are emerging as potent tools for a wide variety of biomedical applications. The aim of this study was to develop a combinatorial approach for enhancing the anticancer efficacy and cellular uptake of DOX.

**Materials and Methods:** ZnO NPs were synthesized by the solvothermal method and were characterized by X-ray diffraction (XRD), dynamic light scattering (DLS) and transmission electron microscopy (TEM). ZnO NPs were dispersed in 10% bovine serum albumin (BSA) and the cytotoxic effect of the resulting ZnO nanofluids was evaluated alone and in combination with DOX on DU145 cells. The influence of ZnO nanofluids on the cellular uptake of DOX and DOX-induced catalase mRNA expression were investigated by fluorescence microscopy and semi-quantitative reverse transcription-polymerase chain reaction (RT-PCR), respectively.

**Results:** The MTT results revealed that ZnO nanofluids decreased the cell viability of DU145 cells in a time- and dose-dependent manner. Simultaneous combination treatment of DOX and ZnO nanofluid showed a significant increase in anticancer activity and the cellular uptake of DOX compared to DOX alone. Also, a time-dependent reduction of catalase mRNA expression was observed in the cells treated with ZnO nanofluids and DOX, alone and in combination with each other.

**Conclusion:** These results indicate the role of ZnO nanofluid as a growth-inhibitory agent and a drug delivery system for DOX in DU145 cells. Thus, ZnO nanofluid could be a candidate for combination chemotherapy.

**Keywords:** Anticancer activity, Catalase, Doxorubicin, Prostate cancer, ZnO nanofluids

### How to cite this article

Soleymani S, Jalal R. ZnO nanofluids for the improved cytotoxicity and cellular uptake of doxorubicin. *Nanomed J.* 2018; 5(1): 27-35. DOI: 10.22038/nmj.2018.05.005

### INTRODUCTION

Doxorubicin (DOX) is a well-known anthracycline drug with therapeutic activity against a variety of human cancers including prostate cancer [1, 2]. The way by which anthracyclines provide their antineoplastic properties has not been totally clarified. The mechanisms discussed are generally based on topoisomerase inhibition, drug intercalation into DNA, membrane interaction, and free radical generation [3-5]. Like other chemotherapeutic agents, the application of DOX in cancer treatment

is limited. The two major limitations that hinder the clinical application of this drug are systemic toxicity and drug resistance [2, 6]. Combination therapy has been extensively developed in order to improve the therapeutic efficacy of chemotherapeutic drugs and reduce the side effects as a result of applying a lower dosage [7, 8].

ZnO nanoparticles (ZnO NPs) have been demonstrated to have a variety of biological properties such as antibacterial, antifungal, photocatalytic, anticancer, and UV blocker activities [9-12]. ZnO NPs are reported to have a strong preferential cytotoxic activity against cancer cells of identical lineage. For example, ZnO NPs showed

\* Corresponding Author Email: [raziieh@um.ac.ir](mailto:raziieh@um.ac.ir)

Note. This manuscript was submitted on December 1, 2017; approved on December 16, 2017

no appreciable cytotoxic effect on resting primary human T lymphocytes at a concentration of  $\leq 5$  mM while a significantly increased ZnO NPs-induced cytotoxicity was observed in the same lineage cancer cells [13, 14]. The mechanisms of cytotoxicity of ZnO NPs are not completely understood, but the increased concentration of  $Zn^{2+}$  (due to ZnO dissociation), reactive oxygen species (ROS) generation and apoptosis are believed to cause cell death [15-17]. Since ZnO NPs are biocompatible and have a few hours of survival time in the body, they can be considered as promising materials for medicinal applications [18]. ZnO NPs are biosafe up to a certain amount, but may be hazardous at higher concentrations. Yang et al. found that no haemolysis occurred in the following exposure to ZnO quantum dots at a concentration of above 1600  $\mu\text{g/ml}$  under in vitro condition [19] and Reddy et al. also showed that ZnO NPs reduced the viability of human T cells at and above 5 mM [20]. At present, it is difficult to determine the threshold limits for various forms of ZnO NPs due to a lack of sufficient data [13-17, 19-24].

Several published studies have revealed that ZnO NPs-DOX complexes or DOX loaded ZnO NPs could have a synergistic cytotoxic activity in cancer cells [25, 26]. Considering the possibility of the combined application of ZnO NPs and chemotherapeutic agents, for the first time we have combined the individual ZnO nanofluids with DOX and not a complex of two agents to inhibit the growth of androgen-independent prostate cancer DU145 cells and increase drug delivery efficiency. Meanwhile, the influence of ZnO nanofluids on the cytotoxicity of DOX in three combination treatments of drugs and nanofluids was investigated by MTT assay. The cellular uptake of DOX and the expression of catalase in DU145 cells were treated simultaneously with ZnO nanofluids and DOX were evaluated by fluorescence microscopy and semi-quantitative RT-PCR, respectively. The results showed the enhanced cytotoxicity and cellular uptake of DOX for DU145 cells in the presence of ZnO nanofluids, suggesting the effective antiproliferative activity of ZnO nanofluids accompanied with DOX.

## MATERIALS AND METHODS

### Preparation of ZnO NPs

Zinc acetate dehydrate (0.001 mol) was dissolved in 80-90 ml of deionized water and then it was diluted to 920 ml. 80 ml of sodium hydroxide (0.02 M). It was slowly added to the zinc acetate

dehydrate solution under magnetic stirring at  $0^\circ\text{C}$  and a transparent  $Zn(OH)_4^{2-}$  solution was formed. The mixture was incubated into a water bath at  $65^\circ\text{C}$  for 2 h and at ambient temperature for 3 days. After that, the white precipitate was collected by centrifugation and it was washed twice with deionized water and ethanol for several times. Then, it was dried in a vacuum oven at  $40^\circ\text{C}$  for 10 h [27]. The synthesized ZnO NPs were characterized by a Bruker Axs D8 ADVANCE diffractometer (Ettlingen, Germany) with Cu K $\alpha$  radiation ( $\lambda = 0.15406$  nm). The transmission electron microscopy (TEM) was recorded by LEO 912AB OMEGA microscope (Massachusetts, USA) operating at 120 kV for the samples. The average particle size was calculated with the Digimizer software.

### Preparation of ZnO nanofluids

Suspensions of ZnO NPs in deionized water were prepared in continuous stirring conditions for 30 min. In order to enhance the stability of the suspension, 10% bovine serum albumin (BSA) was used as a dispersant [28]. Finally, the aqueous solution of the nanoparticles was mixed with the aid of a magnetic stirrer for 4 h. In every sample, the weight ratio of the dispersant to the NPs was kept as 10:1. A nanoparticle size analyzer (Cordouan-Vasco, Pessac France) was used to determine the particle size distribution (PSD).

### Cell culture

The human prostate cancer cell line, DU145, was obtained from American Type Culture Collection (Rockville, MD). Human foreskin fibroblast cells (HFF) was a gift from Tissue Engineering Laboratory in the Department of Biology, Ferdowsi University of Mashhad. RPMI-1640 medium, DMEM medium, penicillin-streptomycin and fetal bovine serum (FBS) were supplied from Biosera, UK. The human prostate cancer cell line, DU145, was cultured in RPMI 1640 medium supplemented with 10% FBS and penicillin-streptomycin at  $37^\circ\text{C}$  in a humidified atmosphere containing 5%  $\text{CO}_2$ .

### Cytotoxicity assays

DU145 cells were seeded in 96-well plates at a density of  $1 \times 10^4$  cells/cm $^2$  and were incubated for 48 h at  $37^\circ\text{C}$  in a 5%  $\text{CO}_2$  humidified environment. Then, the cells were treated BSA alone (10% w/v, control), nanofluids containing different concentrations of ZnO NPs (15.6-250  $\mu\text{g/ml}$ ) which were dispersed in 10% BSA, or DOX (0.05-500  $\mu\text{M}$ )

alone for 24, 48, and 72 h. Each treatment and time point was done at least in triplicate. Controls were cultivated under the same conditions with no addition of ZnO NPs and DOX. Cell viability was measured by MTT (3-(4, 5-Dimethylthiazol-2-yl)-2,5-Diphenyltetrazolium Bromide, Sigma-Aldrich) assay. After the treatment period, 20  $\mu$ l of MTT (5 mg/ml in PBS) was added to each well and it was incubated in 5% CO<sub>2</sub> at 37 °C for 4 h. Then the cells were treated with 150  $\mu$ l of dimethyl sulfoxide (DMSO) and the optical absorbance at 570 nm was recorded using ELx800 Absorbance Microplate Reader (BioTek Instruments, Winooski, VT, USA). The viable cells of the treated group were expressed as follows (Eq. 1):

$$\text{Cell Viability (\%)} = \frac{[A]_{\text{sample}}}{[A]_{\text{control}}} \times 100$$

Where [A] represents the light absorbance at 570 nm. The inhibitory concentration 50 (IC<sub>50</sub>) for ZnO nanofluids and DOX was determined from dose-response curves (cell viability% vs concentration).

According to the above experimental results, the growth-inhibitory effects of combinations of 15.6 and 31.2  $\mu$ g/ml ZnO nanofluids with 0.05 and 0.5  $\mu$ M DOX versus each agent alone were evaluated. Two days after initial seeding, the cells were treated with DOX or ZnO nanofluids either alone or first with DOX and then with ZnO nanofluids 24 h later, or vice versa, or a combination of both agents simultaneously for 48 h. In addition, cell viability was assayed by MTT. The overall effects of DOX and ZnO nanofluids combination in DU145 cells were analyzed by the method of Chou-Talalay [29]. The combination index (CI) was calculated according to the classic isobologram equation (Eq. 2):

$$CI = \frac{d_1}{D_2} + \frac{d_2}{D_1}$$

Where d1 is the dose of drug 1 in the presence of drug 2 and vice versa for d2, required to produce x% effect.

D1 and D2 are doses of 1 and 2 drugs alone, respectively, required to produce the same effect. CI was interpreted as follow: CI < 1.0 synergy, CI > 1.0 antagonism and CI = 1 additive.

#### Fluorescence microscopy

For evaluating the role of ZnO nanofluids in the cellular uptake of DOX, 95  $\times$  10<sup>3</sup> cells were seeded in the 6-well plate and were incubated for 24 h at 37 °C in a 5% CO<sub>2</sub> humidified environment. Then, the cells were treated with 31.2  $\mu$ g/ml of ZnO nanofluids and 10  $\mu$ M of DOX simultaneously. We used 10  $\mu$ M of DOX since at lower concentrations, there is no possibility of detecting fluorescence emission [22]. Cell suspensions containing drug or ZnO nanofluids were taken as controls. Six hours after treatment, the cells were collected and analyzed by fluorescence microscopy (Olympus BX51, Tokyo, Japan).

#### RNA extraction and semi-quantitative reverse transcription polymerase chain reaction (RT-PCR)

DU145 cells were cultured at a density of 10<sup>6</sup> cells per T25 flask for 48 h in RPMI 1640 medium. The cells were treated with ZnO nanofluids (31.2  $\mu$ g/ml) and DOX (0.5  $\mu$ M) separately and simultaneously. After the designated times (3, 6, and 48 hours) of treatment, the total RNA was extracted from cells with RNX plus kit according to the protocol described by the supplier (CinnaGen, Iran). Semi-quantitative RT-PCR was performed using oligo (dT) primer in 20  $\mu$ l volume. The reverse transcription polymerase chain reaction (RT-PCR) reaction was done with 2.0  $\mu$ g of total RNA, 1.0  $\mu$ l of oligo (dT) primer (20  $\mu$ M), 2.0  $\mu$ l of dNTPs (10 mM), 4.0  $\mu$ l buffer (5X), and RNase-free water. After incubation of the mixture at 70 °C for 5 min, the reverse transcription was carried out in the presence of 1.0  $\mu$ l of M-MLV Reverse Transcriptase (200 U/ $\mu$ l) at 42 °C for 60 min and it was terminated at 70 °C for 10 min. PCR amplification was performed on a thermal cycler (Biometra, Germany).

Glyceraldehyde 3- phosphate dehydrogenase (GAPDH) gene was used as an internal standard to monitor the loading variations.

Table 1. Primer sequences of genes used in this study

| Gene name | Gene Bank ID | Primer sequences   | Size (bp) |
|-----------|--------------|--|-----------|
| Catalase  | NM001752.2   | F:5'-TCATGACATTTAATCAGGCA-3'<br>R:5'-GTGTCAGGATAGGCAAAAAG-3'   | 235       |
| GAPDH     | NM002046     | F:5'-GAGCCACATCGCTCAGACAC-3'<br>R:5'CATGTAGTTGAGGTCAATGAAGG-3' | 150       |

The primer sequences of amplified genes and the expected sizes of the PCR products are shown in Table 1. For catalase gene, 1.0  $\mu$ l of the reverse transcription product was amplified in a 25  $\mu$ l mixture containing 0.4  $\mu$ l of Taq DNA polymerase (5 U/ $\mu$ l), 2.5  $\mu$ l PCR buffer (10X), 2.0  $\mu$ l  $MgCl_2$  (25 mM), 0.5  $\mu$ l dNTPs (10 mM), and 2.0  $\mu$ l of each primer (100  $\mu$ M). Amplification conditions were: 5 min at 95  $^{\circ}C$  for the initial denaturation step followed by 30 cycles at 94  $^{\circ}C$  for 1 min, then at 59  $^{\circ}C$  for 1 min, then at 72  $^{\circ}C$  for 1 min and then at 72  $^{\circ}C$  for 10 min.

For the GAPDH gene, PCR was carried out on 1.0  $\mu$ l of the reverse transcription product in a 20  $\mu$ l volume containing 0.2  $\mu$ l Taq DNA polymerase (5 U/ $\mu$ l), 2.0  $\mu$ l PCR buffer (10X), 1.2  $\mu$ l  $MgCl_2$  (25 mM), 0.4  $\mu$ l dNTPs (10 mM), and 0.5  $\mu$ l of each primer (100  $\mu$ M). The PCR conditions were 5 min at 94  $^{\circ}C$ , then 25 cycles at 94  $^{\circ}C$  for 30 s, then at 60  $^{\circ}C$  for 30 s, then at 72  $^{\circ}C$  for 30 s and then at 72  $^{\circ}C$  for 10 min. The amplified cDNA products were electrophoresed on 1.5% agarose gel and were visualized by ethidium bromide staining and UV transilluminator system (Celltoc-illu, Korea).

#### Statistical and densitometry analysis

The results of cell viability are expressed as mean  $\pm$  standard error mean (SEM). Every experiment was repeated for at least three independent times. All data were analyzed utilizing one-way ANOVA Tukey post-test (SPSS software) to determine the statistical significance.  $p$  values  $< 0.05$  were significant statistically. For analysing catalase and GAPDH mRNA expression results, the mean density of each band was evaluated with Non-linear Dynamics of the TotalLab TL120. Densitometry data were compared with control treatment. Changes in mRNA expression were also evaluated.

## RESULTS

#### Characterizations of ZnO nanoparticles

The X-ray diffraction patterns (XRD) of ZnO NPs powder are shown in Fig 1A. These patterns display the hexagonal wurtzite structure of ZnO NPs. All of the reflections from the peaks (1 0 0), (0 0 2), (1 0 1), (1 0 2), (1 1 0), (1 0 3), (2 0 0), (1 1 2), (2 0 1), (0 0 4) and (2 0 2) can be indexed to the known hexagonal wurtzite structure of ZnO with lattice constants of  $a = b = 3.242 \text{ \AA}$  and  $c = 5.205 \text{ \AA}$ . These match well with those in the JCPDS card (Joint Committee on Powder Diffraction Standards, Card No. 89-1397). The strong intensity and the narrow width of ZnO diffraction peaks indicated that the resulting products were with high crystalline.

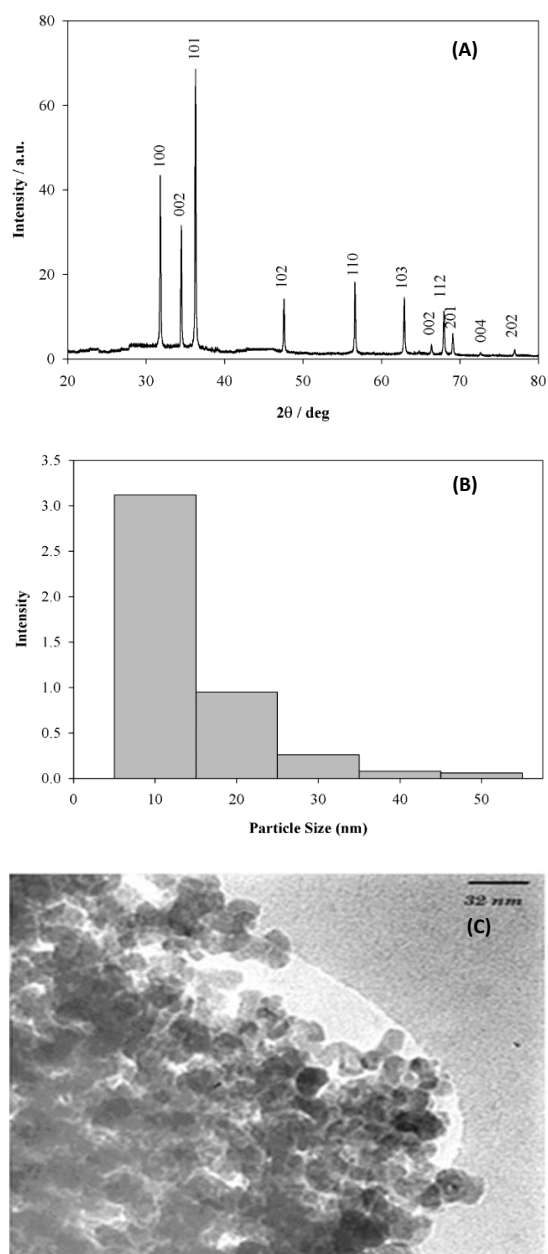


Fig 1. Characterizations of ZnO nanoparticles. X-ray diffraction patterns (A), Particle size distribution of ZnO nanoparticles (B), TEM image (C)

Particle size distribution of ZnO nanofluids is shown in Fig 1B according to its intensity. ZnO NPs with the average size of 10 nm had the most abundance among other nanoparticles with different particle sizes. The TEM image of the particles is depicted in Fig 1C.

The mean size of ZnO particles was calculated to be 8-10 nm. This value matches well with that obtained by particle size distribution.

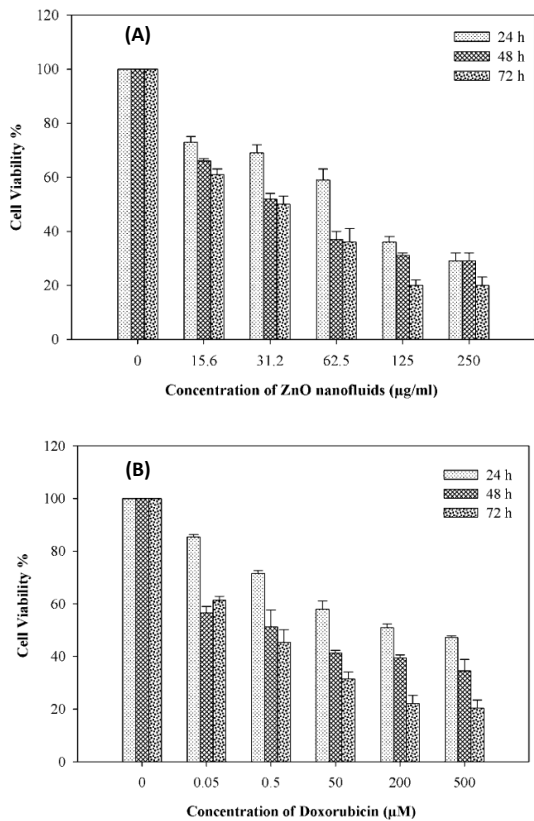


Fig 2. Cytotoxicity. Influence of ZnO nanofluids (A) and doxorubicin (B) on DU145 cell viability

Table 2. Estimated IC50 values for doxorubicin (DOX) and ZnO nanofluids (ZnO NFs) against DU145 cells for 24, 48 and 72 h

| Time (h) | DOX (µM) | ZnO NFs (µg/ml) |
|----------|----------|-----------------|
| 24       | 263.0    | 67.6            |
| 48       | 1.0      | 35.5            |
| 72       | 0.4      | 28.8            |

### Cytotoxicity

First, we investigated the cytotoxic effect of ZnO nanofluids and DOX on DU145 cell growth. The results of MTT assay showed that ZnO nanofluids inhibited cell growth in a time- and dose-dependent manner, accounting for 27.1–70.8, 34.4–71.1, and 39.5–79.8% inhibition in 24, 48 and 72 h from lower to upper concentrations, respectively (Fig 2A). This significant level of cytotoxicity was in agreement with others who had shown that ZnO NPs have toxic dose-dependent effect on cancer cells [18, 22]. Similarly, treatment with DOX alone caused a reduction in dose-dependent growth of DU145 cells, accounting for 14.7–52.8, 43.4–65.5, and 38.6–79.6% inhibition in 24, 48 and 72 h, respectively from lower to upper concentrations (Fig 2B). The estimated IC<sub>50</sub> values of ZnO NPs and DOX against DU145 cells are given in Table 2.

Low concentrations of ZnO nanofluids (15.6 and 31.2 µg/ml) and DOX (0.05 and 0.5 µM) had no significant effect on the cell viability of HFF cells.

In the combination experiment, we used nanofluids containing 31.2 and 15.6 µg/ml concentrations of ZnO nanofluids in combination with 0.5 and 0.05 µM doses of DOX. Cell viabilities were compared with each other in three combination treatments of drug and nanofluids. As it is shown in Table 3, there are significant reductions of cell viability in all combination treatments as compared to single-agent treatments (Fig 2) ( $p < 0.05$ ). The cell viability was significantly reduced in the increased concentration of nanofluids and/or drug when DU145 cells were first treated with

Table 3. Cell viability percentage of DU145 cells in combination treatment of ZnO nanofluids and doxorubicin

| DOX (µM) | ZnO NFs (µg/ml) | DOX / ZnO NFs  | ZnO NFs / DOX | DOX + ZnO NFs |
|----------|-----------------|----------------|---------------|---------------|
| 0.05     | 15.6            | 18.20 ± 2.70** | 34.60 ± 5.50  | 45.05 ± 1.20  |
|          | 31.2            | 16.73 ± 2.02   | 22.32 ± 4.30  | 17.50 ± 3.18  |
| 0.5      | 15.6            | 16.40 ± 0.30*  | 28.83 ± 3.90  | 16.03 ± 0.36* |
|          | 31.2            | 15.50 ± 2.37   | 13.13 ± 1.64  | 10.30 ± 0.56  |

DOX / ZnO NFs: DU145 cells were first treated with doxorubicin for 24 hours and then treated with ZnO nanofluids for 24 hours

ZnO NFs / DOX: DU145 cells were first treated with ZnO nanofluids for 24 hours and then treated with doxorubicin for 24 hours

DOX + ZnO NFs: DU145 cells were treated with combination of doxorubicin and ZnO nanofluids for 48 hours. (\* $p < 0.05$  vs. ZnO NFs (15.6 µg/ml) / DOX (0.5 µM), \*\* $p < 0.01$  vs. DOX (0.05 µM) + ZnO NFs (15.6 µg/ml)). DOX: Doxorubicin, ZnO NFs: ZnO nanofluids

nanofluids and were treated with DOX 24 h later, in totally 48 h ( $p < 0.05$ ).

No dose-dependent reduction of cell viability was observed in cells treated with DOX for 24 h, followed by ZnO nanofluids for another 24 h. The addition of both agents together for 48 h resulted in a significant reduction of cell viability ( $p < 0.05$ ) and the cell viability was reduced with increasing nanofluids and drug concentrations. The CI value for the simultaneous combination was 0.336, indicating synergistic interaction of DOX and ZnO nanofluids.

The results of this study demonstrated that there is no significant reduction of cell viability between different combination treatments of 31.2  $\mu\text{g/ml}$  of nanofluids with either 0.05 or 0.5  $\mu\text{M}$  of drug. Comparison of cell viability in three combination treatments of 0.05  $\mu\text{M}$  of drug and 15.6  $\mu\text{g/ml}$  of nanofluids showed that there are significant differences between cell viabilities when DU145 cells are first treated with drug

and are treated with nanofluids after 24 h in comparison with the other two states ( $p < 0.05$ ).

Concentrations of 0.5  $\mu\text{M}$  of drug and 15.6  $\mu\text{g/ml}$  nanofluids in simultaneous treatment and/or first 24 hours of treatment with drug and the second 24 hours treatment with nanoparticles showed a significant reduction in cell viability in comparison with other states ( $p < 0.05$ ).

#### Cellular uptake of DOX in the presence of ZnO nanofluids

The potential effect of ZnO nanofluids on the drug uptake of DU145 cells has been investigated by using inverted fluorescence microscopy. As it is shown in Fig 3, the accumulation of DOX into DU145 cells was increased in the presence of ZnO nanofluids.

#### Gene expression analysis

To investigate the oxidative stress produced by DOX and ZnO nanofluids as a mechanism of cellular toxicity, DU145 cells were treated with 31.2  $\mu\text{g/ml}$  of ZnO nanofluids and 0.5  $\mu\text{M}$  of drug either alone or simultaneously.

The expression of catalase mRNA and glyceraldehyde-3-phosphate dehydrogenase (GAPDH), as an internal control was determined by semi-quantitative RT-PCR after 3, 6 and 48 h of treatment (Fig 4). The expression level of catalase after 3 and 6 h of treatment with drug alone remained unchanged in comparison with controlled untreated cells.

In contrast, 3 and 6 h of treatment with ZnO nanofluids alone or simultaneously with DOX caused

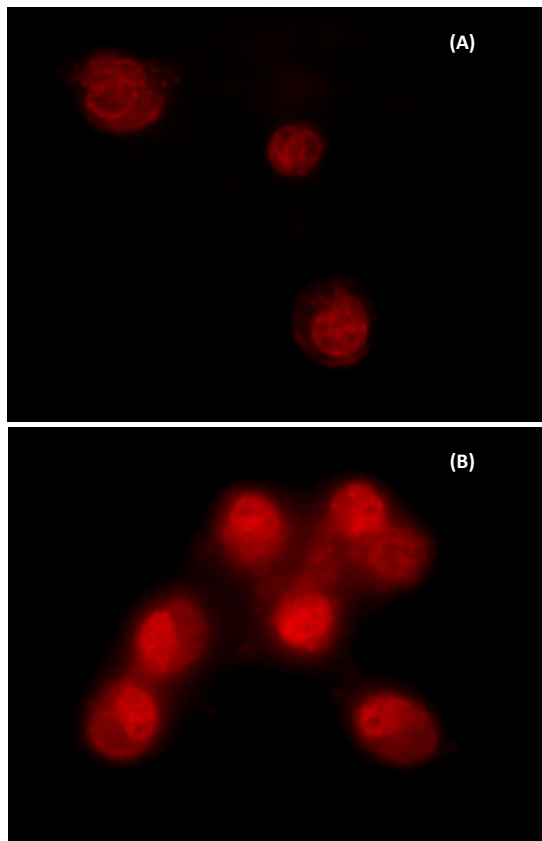


Fig 3. Influence of ZnO nanofluids on cellular uptake of doxorubicin. Inverted fluorescence micrographs of DU145 cells after incubation with 10  $\mu\text{M}$  doxorubicin alone (A) and combination with 31.2  $\mu\text{g/ml}$  ZnO nanofluids (B)

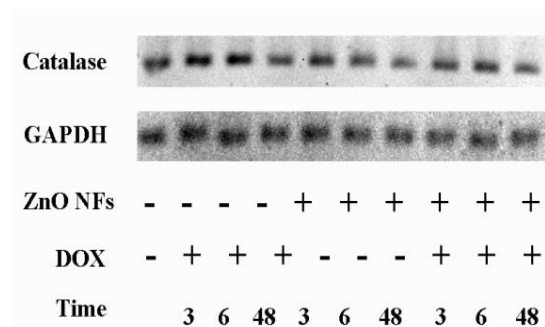


Fig 4. Gene expression analysis. Expression of catalase and GAPDH mRNA in human DU145 prostate cancer cells by RT-PCR after treatment with doxorubicin (0.5  $\mu\text{M}$ ) and ZnO nanofluids (31.2  $\mu\text{g/ml}$ ) either alone or simultaneously for 3, 6, and 48 h.

DOX: Doxorubicin, ZnO NFs: ZnO nanofluids

a decrease of about 25% in mRNA expression of catalase in comparison with the controlled cells. Forty-eight hours of treatment of DU145 cells with ZnO nanofluids alone and in combination with drug resulted in a significant reduction of catalase mRNA levels compared to the controlled cells, whereas the expression level of catalase gene did not significantly change in combined treatment compared with DOX alone.

## DISCUSSION

Doxorubicin causes high toxicity in normal tissues during treatment in an advanced stage of prostate cancer as well as other cancers [30]. Combination chemotherapy has received more attention for the purpose of finding compounds with a known mechanism of action that could increase the therapeutic index of clinical anticancer drugs [31].

Combination of DOX with other agents such as small TGF- $\beta$  inhibitor, selenium, and alphatocopheryl succinate were also investigated. The combination treatment was found to have the potential to reduce the dose and side effects of DOX [6, 31, 32]. Since the unique properties of biocompatible nanomaterials may play an important role in the possible biomedical application, we have evaluated the cytotoxic activity of DOX in the presence of ZnO nanofluids on DU145 cells in this study. ZnO NPs were found to induce toxicity in a cell-specific and proliferation-dependent manner with rapidly dividing and quiescent cells being the most and least sensitive ones, respectively [13]. The marked difference in cytotoxic response between cancer cells and their normal counterparts suggests an exciting potential for ZnO NPs as an alternative to cancer chemotherapy.

Several studies have showed that ZnO NPs can enhance the cytotoxic effect of some chemotherapy agents. Guo et al. (2008) found that the combination of the different size ZnO NPs and daunorubicin under UV irradiation could have a synergistic cytotoxic effect on leukemia cancer cells. They observed that ZnO NPs could effectively enhance the accumulation of daunorubicin in drug-resistant cancer cells [21]. Kim et al. demonstrated that DOX-ZnO nanocomplexes could act as an efficient drug delivery system for importing DOX into SMMC-7721 cells and enhancing its potential chemotherapy efficiency by increasing the intracellular concentration of DOX [33]. The

influence of ZnO NPs on the cytotoxicity of DOX in prostate cancer cells has not been addressed. In the present study, combination treatment resulted in a significant increase in cytotoxic activity of DOX as compared to the single agent ( $p < 0.001$ ). Our observations demonstrated that using a combination approach of ZnO nanofluids with DOX could improve the cellular toxicity of DOX. Thus, the use of ZnO nanofluids and DOX combination therapy could be a promising therapeutic strategy for the treatment of prostate cancer and it will possibly have fewer adverse side effects compared to DOX therapy alone.

Catalase is one of the key components of the antioxidant defense system to prevent the damage from ROS and its expression is thought to be critical for ROS homeostasis. Induction of catalase by oxidative stress depends on the cell line and toxic agents [25, 34]. The generation of ROS is one of the earliest biochemical changes in cancer cells. Beyond ROS involvement in cancer initiation and progression, some anticancer drugs can increase ROS level and inhibit tumour cell growth [25]. Generation of ROS and induction of apoptosis are important determinants of DOX and ZnO NPs cytotoxicity [34, 35]. The effect of DOX on the activity of catalase and its gene expression in different cells has been reported, but with inconsistent results. Catalase expression and its activity were found to increase in DOX resistant K562 and SKVLB cells, whereas a dramatic reduction in catalase was observed in DOX-resistant variant of human breast cancer cell line MCF-7 and acute myeloid leukemia (AML)-2/DX100 [36-38]. The different results of various studies may in part be due to the differences in the cell types and the techniques used. In previous studies, the changes of catalase activity were investigated in response to ZnO NPs [39]. Akhtar et al. (2012) investigated the cytotoxicity of ZnO NPs against three types of cancer cells (human hepatocellular carcinoma HepG2, human lung adenocarcinoma A549, and (BEAS-2B) human bronchial epithelial and two primary rat cells (astrocytes and hepatocytes) [40]. Their results showed that the activity of catalase was significantly lower in ZnO NP-treated cells compared with untreated cells. Wang et al. (2009) found that ZnO NPs significantly diminished the activity of catalase in A549 cells [24].

The influence of ZnO nanofluids in combination with DOX on catalase mRNA expression in prostate cancer cells has not been investigated before. A

significant decrease in catalase mRNA level was detected in cells treated with ZnO nanofluids alone or in combination with DOX in a time-dependent manner. Certainly, the mechanism of catalase expression changes needs further investigation to determine.

## CONCLUSION

The results of this study showed that ZnO nanofluids could act as an efficient factor to enhance the cytotoxic effect of DOX and the uptake of drug in cancer cells, which indicates the potential of ZnO nanofluids to improve DOX efficiency in the growth inhibition of prostate cancer cells. This observation suggests that the combination of ZnO nanofluids with conventional chemotherapy will improve the therapeutic outcomes of tumors.

## ACKNOWLEDGMENT

This work was supported by Ferdowsi University of Mashhad, under grant number 3/17259.

## CONFLICT OF INTEREST

The authors declare no conflicts of interests.

## REFERENCES

- Lüpertz R, Wätjen W, Kahl R, Chovolou Y. Dose- and time-dependent effects of doxorubicin on cytotoxicity, cell cycle and apoptotic cell death in human colon cancer cells. *Toxicology*. 2010; 271(3): 115-121.
- Tyagi AK, Singh RP, Agarwal C, Chan DCF, Agarwal R. Silibinin strongly synergizes human prostate carcinoma DU145 cells to doxorubicin-induced growth inhibition, G2-M arrest, and apoptosis. *Clin Cancer Res*. 2002; 8(11): 3512-3519.
- Muindi JR, Sinha BK, Gianni L, Myers CE. Hydroxyl radical production and DNA damage induced by anthracycline-iron complex. *FEBS Lett*. 1984; 172(2): 226-230.
- Siegfried JA, Kennedy KA, Sartorelli AC, Tritton TR. The role of membranes in the mechanism of action of the antineoplastic agent adriamycin. Spin-labeling studies with chronically hypoxic and drug-resistant tumor cells. *J Biol Chem*. 1983; 258(1): 339-343.
- Wagner BA, Evig CB, Reszka KJ, Buettner GR, Burns CP. Doxorubicin increases intracellular hydrogen peroxide in PC3 prostate cancer cells. *Arch Biochem Biophys*. 2005; 440(2): 181-190.
- Zhang X, Peng X, Yu W, Hou S, Zhao Y, Zhang Z, Huang X, Wu K. Alpha-tocopheryl succinate enhances doxorubicin-induced apoptosis in human gastric cancer cells via promotion of doxorubicin influx and suppression of doxorubicin efflux. *Cancer Lett*. 2011; 307(2): 174-181.
- Figg WD, Arlen P, Gulley J, Fernandez P, Noone M, Fedenko K, Hamilton M, Parker C, Kruger EA, Pluda J, Dahut WL. A randomized phase II trial of docetaxel (taxotere) plus thalidomide in androgen-independent prostate cancer. *Semin in Oncol*. 2001; 28(4 Suppl 15): 62-66.
- Vimala K, Sundarraj S, Paulpandi M, Vengatesan S, Kannan S. Green synthesized doxorubicin loaded zinc oxide nanoparticles regulates the Bax and Bcl-2 expression in breast and colon carcinoma. *Process Biochem*. 2014; 49(1): 160-172.
- Huang W-J, Fang G-C, Wang C-C. A nanometer-ZnO catalyst to enhance the ozonation of 2, 4, 6-trichlorophenol in water. *Colloids Surf A Physicochem Eng Asp*. 2005; 260(1): 45-51.
- Parvin T, Byrappa K, Phanichphant S, Gomez Morales J, Ahmed Ibrahim I, Somashekar R, Ananda S. Hydrothermal synthesis and characterisation of tin doped ZnO polyscale crystals with hexylamine additive. *Mater Res Innov*. 2012; 16(1): 25-29.
- Premanathan M, Karthikeyan K, Jeyasubramanian K, Manivannan G. Selective toxicity of ZnO nanoparticles toward Gram-positive bacteria and cancer cells by apoptosis through lipid peroxidation. *Nanomedicine*. 2011; 7(2): 184-192.
- Sánchez L, Domènech X. Degradation of 2, 4-dichlorophenoxyacetic acid by in situ photogenerated Fenton reagent. *Electrochim Acta*. 1996; 41(13): 1981-1985.
- Hanley C, Layne J, Punnoose A, Reddy KM, Coombs I, Coombs A, Feris K, Wingett D. Preferential killing of cancer cells and activated human T cells using ZnO nanoparticles. *Nanotechnology*. 2008; 19(29): 295103.
- Hanley C, Thurber A, Hanna C, Punnoose A, Zhang J, Wingett DG. The influences of cell type and ZnO nanoparticle size on immune cell cytotoxicity and cytokine induction. *Nanoscale Res Lett*. 2009; 4(12): 1409-1420.
- Rasmussen JW, Martinez E, Louka P, Wingett DG. Zinc oxide nanoparticles for selective destruction of tumor cells and potential for drug delivery applications. *Expert Opin Drug Deliv*. 2010; 7(9): 1063-1077.
- Sharma V, Shukla RK, Saxena N, Parmar D, Das M, Dhawan A. DNA damaging potential of zinc oxide nanoparticles in human epidermal cells. *Toxicol Lett*. 2009; 185(3): 211-218.
- Xia T, Kovochich M, Brant J, Hotze M, Sempf J, Oberley T, Sioutas C, Yeh JI, Wiesner MR, Nel AE. Comparison of the abilities of ambient and manufactured nanoparticles to induce cellular toxicity according to an oxidative stress paradigm. *Nano Lett*. 2006; 6(8): 1794-1807.
- Zhou J, Xu NS, Wang ZL. Dissolving behavior and stability of ZnO wires in biofluids: a study on biodegradability and biocompatibility of ZnO nanostructures. *Adv Mater*. 2006; 18(18): 2432-2435.
- Yang Y, Lan J, Xu Z, Chen T, Zhao T, Cheng T, Shen J, Lv S, Zhang H. Toxicity and biodistribution of aqueous synthesized ZnS and ZnO quantum dots in mice. *Nanotoxicology*. 2014; 8(1): 107-116.
- Reddy KM, Feris K, Bell J, Wingett DG, Hanley C, Punnoose A. Selective toxicity of zinc oxide nanoparticles to prokaryotic and eukaryotic systems. *Appl Phys Lett*. 2007; 90(21): 213902.
- Guo D, Wu C, Jiang H, Li Q, Wang X, Chen B. Synergistic cytotoxic effect of different sized ZnO nanoparticles and daunorubicin against leukemia cancer cells under UV irradiation. *J Photochem Photobiol B*. 2008; 93(3): 119-126.
- Hackenberg S, Scherzed A, Harnisch W, Froelich K, Ginzkey C, Koehler C, Hagen R, Kleinsasser N. Antitumor activity of photo-stimulated zinc oxide nanoparticles combined with paclitaxel or cisplatin in HNSCC cell lines. *J Photochem Photobiol B*. 2012; 114: 87-93.
- Nair S, Sasidharan A, Divya Rani VV, Menon D, Nair



- S, Manzoor K, Raina S. Role of size scale of ZnO nanoparticles and microparticles on toxicity toward bacteria and osteoblast cancer cells. *J Mater Sci Mater Med.* 2009; 20(1): 235-241.
24. Wang H, Wingett D, Engelhard MH, Feris K, Reddy KM, Turner P, Layne J, Hanley C, Bell J, Tenne D, Wang C. Fluorescent dye encapsulated ZnO particles with cell-specific toxicity for potential use in biomedical applications. *J Mater Sci Mater Med.* 2009; 20(1): 11-22.
25. Deng Y, Zhang H. The synergistic effect and mechanism of doxorubicin-ZnO nanocomplexes as a multimodal agent integrating diverse anticancer therapeutics. *Int J Nanomedicine.* 2013; 8: 1835-1841.
26. Liu J, Ma X, Jin S, Xue X, Zhang C, Wei T, Guo W, Liang XJ. Zinc oxide nanoparticles as adjuvant to facilitate doxorubicin intracellular accumulation and visualize pH-responsive release for overcoming drug resistance. *Mol Pharm.* 2016; 13(5): 1723-1730.
27. Moosavi M, Goharshadi EK, Youssefi A. Fabrication, characterization, and measurement of some physicochemical properties of ZnO nanofluids. *Int J Heat Fluid Flow.* 2010; 31(4): 599-605.
28. Tantra R, Tompkins J, Quincey P. Characterisation of the de-agglomeration effects of bovine serum albumin on nanoparticles in aqueous suspension. *Colloids Surf B Biointerfaces.* 2010; 75(1): 275-281.
29. Chou TC. Drug combination studies and their synergy quantification using the Chou-Talalay method. *Cancer Res.* 2010; 70(2): 440-446.
30. Raghavan D, Koczwarra B, Javle M. Evolving strategies of cytotoxic chemotherapy for advanced prostate cancer. *Eur J Cancer.* 1997; 33(4): 566-574.
31. Von Hoff DD, Layard MW, Basa P, Davis JHL, Von Hoff AL, Rozencweig M, Muggia FM. Risk factors for doxorubicin-induced congestive heart failure. *Ann Intern Med.* 1979; 91(5): 710-717.
32. Bandyopadhyay A, Wang L, Agyin J, Tang Y, Lin S, Yeh IT, De K, Sun LZ. Doxorubicin in combination with a small TGFbeta inhibitor: a potential novel therapy for metastatic breast cancer in mouse models. *PLoS One.* 2010; 5(4): 0010365.
33. Kim AR, Ahmed FR, Jung GY, Cho SW, Kim DI, Um SH. Hepatocyte cytotoxicity evaluation with zinc oxide nanoparticles. *J Biomed Nanotechnol.* 2013; 9(5): 926-929.
34. Dröge W. Free radicals in the physiological control of cell function. *Physiol Rev.* 2002; 82(1): 47-95.
35. Tsang WP, Chau SP, Kong SK, Fung KP, Kwok TT. Reactive oxygen species mediate doxorubicin induced p53-independent apoptosis. *Life Sci.* 2003; 73(16): 2047-2058.
36. Akman SA, Forrest G, Chu F-F, Esworthy RS, Doroshov JH. Antioxidant and xenobiotic-metabolizing enzyme gene expression in doxorubicin-resistant MCF-7 breast cancer cells. *Cancer Res.* 1990; 50(5): 1397-1402.
37. Kalinina E, Chernov N, Saprin A, Kotova YN, Andreev YA, Solomka V, Scherbak NP. Changes in expression of genes encoding antioxidant enzymes, heme oxygenase-1, Bcl-2, and Bcl-xl and in level of reactive oxygen species in tumor cells resistant to doxorubicin. *Biochemistry (Mosc).* 2006; 71(11): 1200-1206.
38. Lee T-B, Moon Y-S, Choi C-H. Histone H4 deacetylation down-regulates catalase gene expression in doxorubicin-resistant AML subline. *Cell Biol Toxicol.* 2012; 28(1): 11-18.
39. Du W, Sun Y, Ji R, Zhu J, Wu J, Guo H. TiO<sub>2</sub> and ZnO nanoparticles negatively affect wheat growth and soil enzyme activities in agricultural soil. *J Environ Monit.* 2011; 13(4): 822-828.
40. Akhtar MJ, Ahamed M, Kumar S, Khan MM, Ahmad J, Alrokayan SA. Zinc oxide nanoparticles selectively induce apoptosis in human cancer cells through reactive oxygen species. *Int J Nanomedicine.* 2012; 7: 845-857.